The American Journal of Pathology, Vol. 176, No. 4, April 2010

DOI: 10.2353/ajpath.2010.090782

Vascular Biology, Atherosclerosis and Endothelium Biology

Histidine-Rich Glycoprotein Modulates the Anti-Angiogenic Effects of Vasculostatin

Philip A. Klenotic,* Ping Huang,† Juan Palomo,‡ Balveen Kaur,§ Erwin G. Van Meir,¶ Michael A. Vogelbaum,‡ Maria Febbraio,* Candece L. Gladson,† and Roy L. Silverstein*

From the Departments of Cell Biology, and Cancer Biology,† and the Brain Tumor and Neuro-Oncology Center,‡ Lerner Research Institute, Cleveland Clinic, Cleveland, Ohio; the Dardinger Laboratory for Neuro-Oncology and Neurosciences,§ the Ohio State University, Columbus, Ohio; and the Department of Neurosurgery, Hematology/Medical Oncology and Winship Cancer Institute,¶ Emory University, Atlanta, Georgia*

Brain angiogenesis inhibitor 1 (BAI1) is a transmembrane protein expressed on glial cells within the brain. Its expression is dramatically down-regulated in many glioblastomas, consistent with its functional ability to inhibit angiogenesis and tumor growth *in vivo*. We have shown that the soluble anti-angiogenic domain of BAI1 (termed Vstat120) requires CD36, a cell surface glycoprotein expressed on microvascular endothelial cells (MVECs), for it to elicit an anti-angiogenic response. We now report that Vstat120 binding to CD36 on MVECs activates a caspase-mediated pro-apoptotic pathway, and this effect is abrogated by histidine-rich glycoprotein (HRGP). HRGP is a circulating glycoprotein previously shown to function as a CD36 decoy to promote angiogenesis in the presence of thrombospondin-1 or −2. Data here show that Vstat120 specifically binds HRGP. Under favorable MVEC growth conditions this interaction allows chemotactic-directed migration as well as endothelial tube formation to persist in *in vitro* cellular systems, and increased tumor growth *in vivo* as demonstrated in both subcutaneous and orthotopic brain tumor models, concomitant with an increase in tumor vascularity. Finally, we show that HRGP expression is increased in human brain cancers, with the protein heavily localized to the basement membrane of the tumors. These data help define a novel angiogenic axis that could be exploited for the treatment of human cancers and other diseases where excess angiogenesis occurs. *(Am J Pathol 2010, 176:2039–2050; DOI: 10.2353/ajpath.2010.090782)*

Angiogenesis is the process through which new blood vessels are formed from pre-existing capillaries. In adulthood the vasculature is normally quiescent, a homeostatic state that is maintained by a precise balance of pro-angiogenic inducers such as vascular endothelial growth factor and anti-angiogenic inhibitors such as thrombospondin (TSP)−1 and −2. This angiostatic balance can be physiologically regulated in favor of new blood vessel formation during processes such as menstruation and wound healing allowing normal tissue regeneration; while pathological disruption of this balance is associated with many disease states, including diabetic retinopathy, atherosclerosis-induced tissue ischemia, chronic inflammation, tumor growth and metastasis, obesity, asthma, and several autoimmune diseases.[1] Therefore, it is extremely important to identify and dissect the pathways involved in vessel growth in both normal and aberrant conditions.

Neovascularization is a major component of malignant tumor growth and many therapeutic strategies have been developed to inhibit tumor angiogenesis, including antibodies or decoys that bind and neutralize vascular endothelial growth factor,[2,3] small molecule inhibitors of growth factor signaling pathways,[4] and peptides based on the anti-angiogenic type I repeat domains (TSR) of TSP-1.[5–7] Studies on the mechanisms of TSP-mediated anti-angiogenesis revealed that the TSR domains play an essential role[8] and that the type B scavenger receptor CD36 functions as the critical endothelial cell surface receptor.[9,10] Using mouse corneal pocket angiogenesis assays we recently demonstrated that CD36 also functions as the receptor for a 120 kDa anti-angiogenic fragment derived from an unrelated TSR-containing protein, Brain Angiogenesis Inhibitor 1 (BAI1). This fragment, known as vasculostatin or Vstat120, suppressed neovessel formation in corneas from wild-type mice yet no effect was observed in CD36 null animals, showing for the first

Supported by National Institutes of Health grants HL67839 (to R.L.S.) and CA86335 (to E.G.V.M.). P.A.K. was supported by the American Heart Association grant 0525334B.

Accepted for publication December 14, 2009.

Address reprint requests to Roy L. Silverstein, M.D., Department of Cell Biology, Lerner Research Institute, Cleveland Clinic, Cleveland, OH 44195. E-mail: silverr2@ccf.org.

time that a TSR-containing protein distinct from TSP-1 and −2 mediates its anti-angiogenic functions through interactions with CD36.[11]

BAI1 is a 1584-aa brain-specific protein predicted to have seven transmembrane segments and a large extracellular domain. The extracellular domain contains an RGD integrin recognition motif, a putative hormone receptor (HomR) domain, and five TSR domains. Its expression is down-regulated in glioblastomas[12] and inversely correlated with vascularity and metastasis in colorectal cancer,[13] consistent with an anti-angiogenic role. Kaur et al[14] have shown that the TSR-containing fragment, Vstat120, was released from the cell membrane via proteolytic cleavage at a G protein–coupled receptor cleavage site and that this fragment inhibited microvascular endothelial cell (MVEC) proliferation, migration, and tube formation equivalent to that seen with full-length BAI1. Strikingly, restoration of Vstat120 expression in human glioma cells suppressed tumorigenicity and vascularity and enhanced animal survival in subcutaneous and orthotopic tumor implantation models in nude mice.[11]

The binding site on CD36 for the TSR domains of TSP-1 and −2 and Vstat120 has been localized to amino acids 93 to 120[11,15,16] within a highly conserved region termed the CLESH domain (*C*D36, *L*IMP2, *E*MP *s*tructural *h*omology – see Figure 1A). CLESH domains are also found in proteins genetically distinct from the CD36 family,[17] including some, such as HIV gp120 and histidine-rich glycoprotein (HRGP) which are known to bind TSP-1. HRGP, a 75-kDa glycoprotein synthesized in the liver, circulates in the blood at moderately high concentrations (approximately 100 to 150 μg/ml), and is secreted from activated platelets. In addition to TSP-1 and −2, it binds a wide range of ligands including divalent metal cations and several components of the provisional matrix laid down by healing wounds and tumors where angiogenesis is prevalent (for review see[18]). It has been implicated in the coagulation and fibrinolytic systems, and high levels have been associated with thrombotic disorders.[19,20] Work in our lab has shown that HRGP acts as a CD36 decoy to promote angiogenesis by binding TSP-1 and −2 and thereby preventing them from binding to CD36 on the endothelial cell surface.[21,22] Because both HRGP and CD36 compete for the identical binding region in TSP-1 and −2, we hypothesized that the relative concentrations of ligands, receptor, and decoy within a given microenvironment would ultimately determine the degree of angiogenesis. Within tumors and other areas of chronic inflammation, HRGP can be released from activated platelets as well as deposited from plasma that gained access via poorly organized hyperpermeable vessels. The angiogenic balance would then be tipped to favor angiogenesis by HRGP binding to TSPs as well as potentially other TSR containing anti-angiogenic proteins.

In this article we show that the CLESH domain of HRGP binds Vstat120 and suppresses its anti-angiogenic activity by reversing inhibition of endothelial cell migration and tube formation. Furthermore, we show in both subcutaneous and orthotopic brain tumor models that HRGP exacerbates glioblastoma tumor growth and enhances tumor vascularity. We also show that the amount of HRGP present in human brain is increased in patients with primary tumors with the protein localized predominantly within the basement membrane. Finally, we offer some insight into the mechanism of action of Vstat120 by showing caspase-3 activation and endothelial cell apoptosis on Vstat120 addition. Together these results suggest that deposition of HRGP into angiogenic microenvironments, perhaps as the result of the inherent "leakiness" of the neo-vasculature and/or of platelet granule release, can modulate the anti-angiogenic processes mediated by the general family of TSR-containing proteins, and may shed light on the mechanism of angiogenesis regulation in the brain.

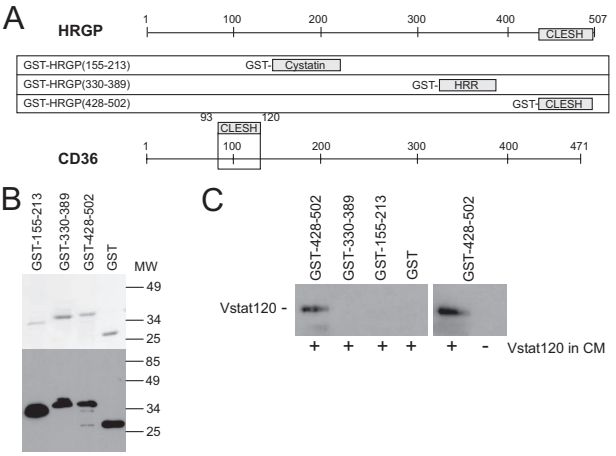

Figure 1. HRGP CLESH domain fusion protein specifically precipitates Vstat120 from tumor cell postculture media. **A:** HRGP/GST fusion proteins. Three recombinant GST fusion proteins were designed using fragments of the HRGP protein spanning amino acids 155 to 213 (within the second cystatin domain), amino acids 330 to 389 (the HRR), and amino acids 428 to 502 (CLESH domain). The linear structure of CD36 with the CLESH domain highlighted is shown below for reference. **B:** Coomassie stained gel (**top panel**) showing the purified GST-HRGP protein fragments after glutathione sepharose chromatography. The **bottom panel** shows Western blot analysis of each fusion protein probed with anti-GST antibody. **C:** Western blot analysis of a GST pull-down assay. The three GST-HRGP fusion proteins and GST alone were bound to glutathione sepharose beads, and CM from LN229V120 glioma cells were added to each sample. Each precipitate was then probed using the Vstat120/BAI1-specific antibody. Vstat120 was only detected when the CLESH domain (HRGP 428 to 502) was used in the pull-down and not the cystatin (HRGP 155 to 213) or the HRR (HRGP 330 to 389) domains. HRGP 428 to 502 only precipitated Vstat120 when CM from Vstat120-transfected LN229 cells (+ lanes) was used. No protein was detected when CM from the nontransfected parent cells (− lane) was used. This is a representative image from $n = 3$ experiments.

Materials and Methods

Antibodies and Reagents

Mouse anti–glutathione *S*-transferase (GST) monoclonal antibody (MAB3317) was purchased from Chemicon International (Millipore – Billerica, MA). Anti-human HRGP monoclonal antibody (MAB1869) was purchased from R&D Systems (Minneapolis, MN) and anti-human N-terminal BAI1 polyclonal antibody was previously described.[14] Rabbit anti-human caspase-3 antibody (#9662) was purchased from Cell Signaling Technology (Beverly, MA). Horseradish peroxidase (HRP)-conjugated anti-rabbit $F(ab')_2$ from donkey, HRP anti-mouse IgG-linked whole

antibody from sheep, and glutathione sepharose used for GST pull-down assays were obtained from GE Health care (Piscataway, NJ). Staining of tumor slides was performed using rabbit anti-vWF and developing antibodies contained in the Blood Vessel Staining Kit Peroxidase System (ECM590) from Chemicon.

Recombinant Fusion Proteins

Three different HRGP fragments spanning amino acids 155 to 213, 330 to 389, and 428 to 502 were cloned by PCR and expressed as recombinant GST fusion proteins in the *E. coli* expression strain Bl21(DE3) using the vector pGEX6P1 (GE Health care). Figure 1A shows their orientation in relationship to full-length HRGP. All constructs were verified by direct nucleotide sequencing. One hundred ml cultures were used for each purification. The GST-HRGP (330 to 389) peptide was soluble whereas the other GST fusion proteins were expressed mainly in inclusion bodies. These were pelleted at 31,000*g* for 30 minutes, washed successively with PBS + 0.1% Triton X-100 and 50 mmol/L NaH_2PO_4, 300 mmol/L NaCl, pH 8.0, then dissolved in 5 ml of 8 mol/L urea, 50 mmol/L Tris-HCl, pH 8.0. After centrifugation to remove insoluble debris the proteins were refolded by dropwise addition into 20 ml of refolding buffer (20 mmol/L Tris-HCl, 5 mmol/L DTT, 1 mmol/L EDTA, pH 9.0). Refolded proteins were then dialyzed to remove remaining urea and centrifuged at 31,000*g* for 30 minutes to remove misfolded protein aggregates. Recombinant proteins were purified by affinity chromatography using glutathione sepharose 4B (GE), dialyzed in 20 mmol/L Tris, pH 8.0, and stored at −20°C. Figure 1B (top) shows by SDS-PAGE that each protein was purified to near homogeneity and migrated at their predicted molecular weight. The fusion proteins were also recognized by Western blot with anti-GST monoclonal antibody (Figure 1B, bottom).

Glioma Cell Lines

Human glioma cells stably transfected with the Vstat120 cDNA (LN229V120) and the non-transfected parental line (LN229) were prepared and maintained as previously described.[14] LN229V120 cells were transfected with cDNA encoding full-length human histidine-tagged HRGP in vector pcDNA6A (Invitrogen, Carlsbad, CA). LN229V120 cells transfected with plasmid vector without the HRGP cDNA was used as a control for non-specific effects of the vector sequence (6A8 line). Cells in 100-mm tissue culture dishes with LN229V120 cells at 80% confluence were transfected with 3 μg of plasmid DNA using the Fugene 6 reagent (Roche, Applied Science, Indianapolis, IN) and established protocol. The cells were put under selection in DMEM media containing 10 ng/ml of blasticidin-HCl. Using filter paper soaked in trypsin solution, single colonies were transferred to a 96-well plate and resistant clones were amplified. Serum-free conditioned media (CM) from 100-mm dishes were collected after 72 hours, and CM proteins were either concentrated in an Amicon Centriprep YM-50, or precipitated by TCA and screened for the presence of full-length HRGP via immunoblot.

Glutathione-S-Transferase Pull-Down Assay

Postculture media from transfected and control LN229 cells were pre-absorbed with 50 μl of glutathione sepharose 4B for 1 hour at 4°C then incubated at 4°C overnight with constant rotation with glutathione sepharose 4B beads bound to the various GST fusion proteins. The mixtures were centrifuged at 100*g* for 1 minute to sediment the beads, then the beads were washed 3× with 5 ml of PBS. Bound proteins were eluted and solubilized in 50 μl of 2× Laemmli sample buffer with 5% β-mercaptoethanol (β-ME) then analyzed by immunoblot using HRP-conjugated secondary antibodies and an ECL chemiluminescent detection system (GE).

Crystal Violet Growth Assay

Cells were seeded onto a 96-well plate at 4000 cells per well in triplicate. At timed points the media was removed, the wells washed with PBS, and 50 μl of crystal violet solution was added for 10 minutes at room temperature. After washing 3× with distilled H_2O and allowed to drain, a 1% SDS (100 μl) solution was added to solubilize the stain for 10 minutes at room temperature on an orbital shaker. On uniform color appearance, the absorbance of each well was read at 570 nm on a spectramax 190 luminometer (MDS Analytical Technologies, Ontario, Canada).

Endothelial Cell Migration Assay

Early passage human dermal microvascular endothelial cells (HDMVECs - passage 3; Lonza, Basel, Switzerland) grown in endothelial growth media (EGM) complete growth medium were used for all studies. In a 24-well tissue culture plate, 500 μl of serum-free media with or without basic fibroblast growth factor (10 ng/ml) was added. A suspension of 5.0×10^5 cells/ml in serum-free media was prepared and 300 μl added to the millicell migration insert (Millipore). To this suspension conditioned media from either Vstat120-transfected cells or Vstat120-transfected cells co-transfected with HRGP was added. The inserts were placed into the migration plate and allowed to migrate for 18 hours at 37°C with 5% CO_2. The media was aspirated and nonmigratory cells were removed with a cotton swab. The membrane was cut away from the insert, placed onto a glass slide coated with DAPI, sealed, and visualized under fluorescence. The number of migrating cells were counted in five random fields per well and results expressed as number of migrating cells per field.

Scratch Wound Assay

HDMVECs were plated onto a 12-well dish and allowed to grow to confluence. After incubation in serum-free media overnight a thin acellular line was made with a sterile 200

μl pipet tip in the middle of the well and the media changed to a 1:1 mix of complete media plus CM from the various transfected LN229 cells (prepared in serum-free DMEM as previously described). The HDMVECs were allowed to incubate overnight at 37°C before cellular migration into the denuded area was assessed by phase contrast microscopy.

Caspase-3 Assay

Confluent monolayers of HDMVECs in six-well dishes were synchronized by incubation overnight in low-serum growth medium (2 ml serum-free EGM + 0.5 ml of complete EGM – Clontech, Mountain View, CA). After washing with PBS, CMs from various LN229 lines were added and incubated at 37°C for 8 hours. The CM-EC supernatants were centrifuged at 1000*g* to pellet the dead cells and cell debris. All but 1 ml of the supernatant was removed. The dead cells were resuspended and the remaining liquid was transferred to a 1.5 ml Eppendorf tube and centrifuged at 17,000*g* for 5 minutes. The dead cells and debris were washed with 750 μl of PBS and centrifuged again at 17,000*g*. The pellet was resuspended in 20 μl of Laemmli sample buffer plus β-ME. The remaining cells on the dish were washed 1× with PBS, the liquid removed, and the cells scraped into 100 μl of sample buffer plus β-ME. Twenty μl was combined with the previous dead cell pellet and loaded onto a 15% SDS-PAGE gel. Both total and cleaved caspase-3 was detected using anti–caspase-3 antibody (Cell Signaling).

Tube Formation Assay

In a 24-well dish, 320 μl of Matrigel (Becton Dickinson Labware, Franklin Lakes, NJ) was added per well and allowed to polymerize for 30 minutes at 37°C. To each well 3×10^4 HDMVECs in complete EGM media mixed 1:1 with serum-free conditioned media from the transfected LN229 cells was added. After 24 hours tube formation was assessed by number of branch points counted using phase contrast microscopy.

Tumor Assays

All animal procedures were conducted in accordance with the Cleveland Clinic Institutional Animal Care and Use Committee.

Subcutaneous Tumor Model

Male athymic nude mice ($n = 4$ mice, 2 tumors per mouse) were injected subcutaneously with 1.5×10^6 of Vstat120-expressing, or Vstat120 and HRGP-expressing LN229 glioma cells. Tumor growth was measured with a caliper 3× per week and tumor volume calculated using the formula $V = 1/2 \times A \times B^2$ with A as the tumor length and B the width. Animals were constantly monitored for overall health and euthanized if adverse effects attributable to tumor burden were noticed. After day 50 mice were euthanized and the tumors harvested for immunohistochemical analysis.

Orthotopic Intracranial Tumor Model

3×10^5 glioma cells were injected into the brains of athymic nude mice (six animals per group). These mice were anesthetized with ketamine and xylazine and secured to a stereotactic frame. A sagittal midline incision was made from 5 mm anterior of the bregma to the occiput. A 2-mm drill was used to make a hole 2.5 mm to the right and 0.5 mm anterior of the bregma. A Hamilton syringe was then lowered 3.5 mm through the skull and raised 0.5 mm to create a pocket for cell implantation. Three μl of the LN229 glioma cells (100,000 cells/μl) were slowly injected into the brain at a rate of one μl per minute. The syringe was kept in place for 5 minutes after injection then slowly retracted to minimize backflow. The surface of the skulls was washed with sterile water and each incision closed with a surgical staple. The mice were monitored daily for adverse effects, and one was sacrificed before the end date due to morbidity.

Histological Analysis

After 9 weeks, the mice were sacrificed and the brains were excised, fixed in formalin, dehydrated in 20% sucrose in PBS, and embedded in OCT compound. Coronal sections were cut at 10 μm and frozen at −80°C. On thawing for 30 minutes at room temperature, sections between 1 mm anterior to 1 mm posterior to the bregma were washed 3× in PBS, then either stained with anti-vWF and anti-rabbit Alexa Fluor 488 antibody (Invitrogen – Carlesbad, CA) then mounted with ProLong Gold antifade reagent with DAPI, or stained with Mayer Hematoxylin (Dako Cytomation – Carpinteria, CA) for 3 minutes. The hematoxylin sections were then washed with H_2O for 15 minutes and stained with Accustain Eosin Y solution (Sigma – Aldrich, St. Louis, MO) for 3 minutes. After a quick rinse in H_2O the sections were dehydrated and mounted with VectaMount permanent mounting medium (Vector Laboratories – Burlingame, CA). Pictures were taken with a camera attached to a Leica DM5000 microscope. The sections with the largest tumor area within 2 mm of the bregma were used for percent area determination and the peripheral regions where there was contact with non-tumorous tissue were assayed for vessel analysis.

Immunohistochemistry of Paraffin Sections

Subcutaneous tumors were fixed in formalin, processed, embedded in paraffin, and sectioned. Transverse sections starting 1 mm from the tumor edge were used for subsequent staining experiments. Sections were deparaffinized, hydrated, and incubated for 20 minutes at 37°C in 0.2 N HCl with 0.4% pepsin. Sections were then stained with anti-vWF IgG or control serum and developed according to the manufactures' instructions (Chemicon Blood Vessel Staining Kit). For studies of human nontumorous brain

and glioblastoma (GBM), 20 normal brain and 18 GBM biopsy samples were stained for HRGP. Formalin-fixed and paraffin-embedded samples were deparaffinized and subjected to antigen retrieval (10 mmol/L sodium citrate, pH 6.0, boiled for 8 minutes followed by a 5 minutes cool down). The samples were blocked for nonspecific peroxidase activity and then blocked for nonspecific avidin activity with the Avidin-Biotin blocking reagent (Vector Laboratories, Burlingame, CA). The tissues were incubated with 0.7 μg/ml anti-HRGP IgG or control IgG (4°C, overnight), reacted with 6 μg/ml biotinylated anti-mouse IgG (2 hours, 22°C), and then reacted with the Avidin-Biotin-Complex (Vector Laboratories). The tissue slides were developed with the DAB substrate, counterstained with hematoxylin, and photographed at 40× magnification using a Leica DMR microscope. Positive staining was graded either wk+, weak intensity; 1+, strong intensity; and 2+, very strong intensity when compared with the IgG control.

Results

Vstat120 Binds to the CLESH Domain of HRGP

To test the hypothesis that the CLESH domain of HRGP can bind specifically to nonthrombospondin family TSR-containing proteins we developed a pull-down assay using recombinant GST fusion proteins bound to sepharose beads as bait and postculture media from Vstat120 cDNA-transfected glioma cells as target. GST fusion peptides containing the three major HRGP structural domains (CLESH, histidine and proline rich regions (HRR), and cystatin) and the CD36 CLESH domain are shown in Figure 1, A and B. Figure 1C shows by immunoblot that the C-terminal HRGP CLESH domain (428 to 502)-containing fusion protein specifically precipitated Vstat120 from the CM, whereas GST alone or fusion proteins containing the HRR domain (330 to 389) or the cystatin domain (155 to 213) did not. Additionally, no Vstat120 was detected in the precipitates from glioma cells transfected with the control plasmid, showing specificity.

Construction of HRGP-Expressing Glioma Cell Lines

To examine the *in vivo* functional relevance of the HRGP-Vstat120 association a cDNA encoding full-length HRGP was stably transfected into LN229Vstat120 cells. These cells were derived from a human glioma and constitutively express Vstat120.[11,14] Figure 2A shows a Western blot for HRGP (top) and Vstat120 (bottom) of CM from several clones and shows that lines 5, 18, 22, and 23 express both proteins, whereas cells transfected with the empty pcDNA6A vector (line 6A8) express Vstat120 but not HRGP. Lines 5, 22, and 23 were expanded and continued to show protein expression through multiple passages. The relative levels of HRGP protein secretion from these cell lines was determined using Western blots of 20-fold concentrated media from cultures maintained in serum-free conditions for 5 days after reaching 80% confluence. Figure 2B shows that lines 5 and 23 have similar expression levels, whereas line 22 produces fivefold more HRGP. Relative concentrations were determined from five separate experiments. The amount of Vstat120 was similar for all lines tested (data not shown). These cloned cell lines allowed us to examine the effects of HRGP on tumor growth and angiogenesis at two different HRGP expression levels.

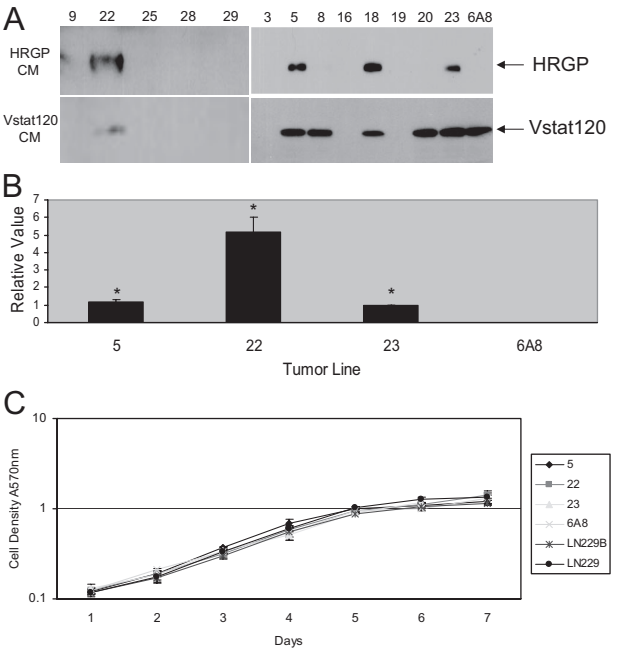

Figure 2. LN229V120 glioma cloned cell lines stably express HRGP. **A:** Western blot of CM from 13 different cloned HRGP LN229V120 glioma lines probed with antibodies to HRGP (**top panel**) and Vstat120 (**bottom panel**). Lines 5, 18, 22, and 23 all showed considerable expression of HRGP while retaining Vstat120 expression. The control line (6A8) was transfected with empty vector and expressed Vstat120, but not HRGP as expected. Other lines either expressed Vstat120 alone 8, 20 or neither protein. 9, 16, 19, 25, 28, 29 **B:** Relative levels of expression of HRGP transfected lines. The amount of CM tested was normalized to total cell number at time of collection. HRGP expression levels in CM were assessed by Western blot and compared with that of line 23. Lines 5 and 23 were almost identical in expression level, whereas line 22 expressed fivefold more compared with the other two ($^*P < 0.002$) **C:** HRGP expression did not have an effect on *in vitro* growth rates. All cells were seeded at the same cell density and proliferation was monitored by crystal violet assay. All lines proliferated at near identical rates and reached plateau at days 6 to 7.

The cloned cell lines were also assessed for *in vitro* growth characteristics using a crystal violet cell proliferation assay. Figure 2C shows a seven-day growth curve for three HRGP-expressing lines along with LN229Vstat120 (LN229B), the empty vector control (6A8), and the untransfected parental LN229 glioma line. All lines tested showed comparable growth rates and reached plateau phase at similar times.

HRGP Reverses the Activity of Vstat120 in Vitro

Angiogenesis can be broken down into several processes, including endothelial cell migration, proliferation, and tube formation, all of which are required for the formation of patent capillaries. The effects of Vstat120 and HRGP were tested on low passage HDMVEC in an endothelial scratch wound assay.[23] This assay provides

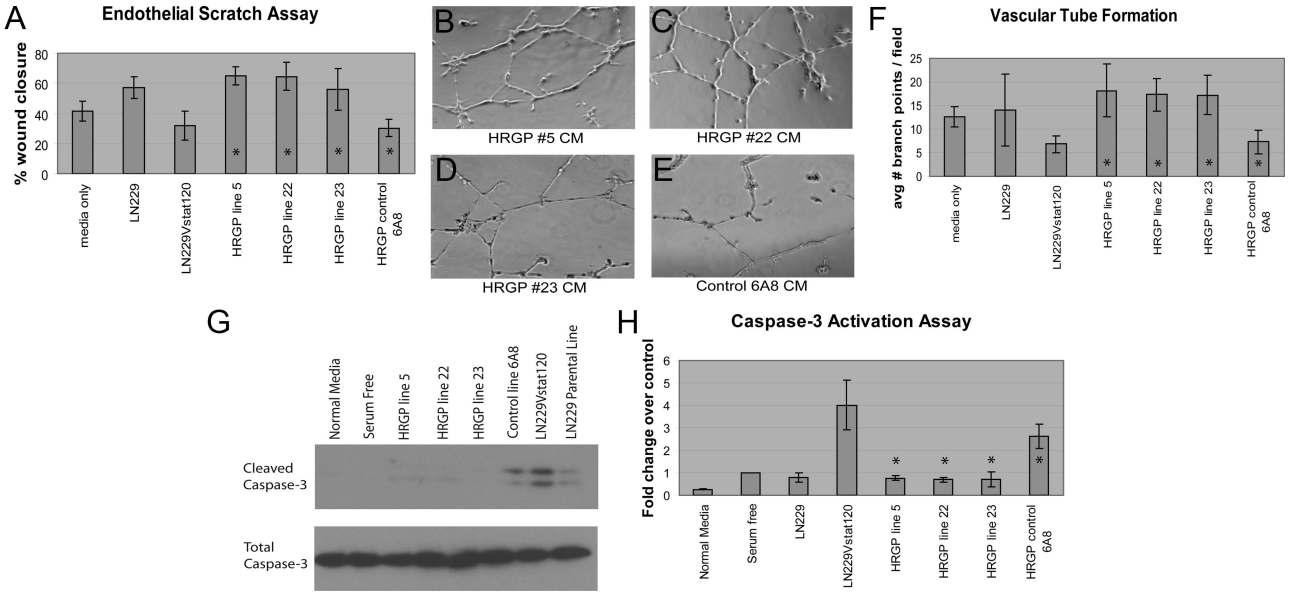

Figure 3. HRGP reverses inhibition of endothelial cell migration and tube formation by Vstat120. **A:** Scratch assays. A scratch was made within a confluent monolayer of HDMVECs and the cells were incubated overnight with normal media (media only – lane 1) showing moderate migratory growth into the acellular area of about 40% total closure. When CM from Vstat120-expressing cells (6A8 – lane 7 and LN229Vstat120 – lane 3) was added, fewer cells were seen migrating from the original cell boundary, especially when compared with the parental LN229 line (lane 2). An average of 30.3% and 31.7% closure, respectively, was calculated for the Vstat120-rich CMs used versus 57% for LN229. When CM from lines expressing both Vstat120 and HRGP (line 5 – lane 4, line 22 – lane 5, and line 23 – lane 6) was added cell migration equal to or greater than cells treated with normal growth media only was seen and approximately doubled that of the 6A8 control. The percent wound was 65.1%, 64.6%, and 56.0% for the three HRGP lines compared with 30.3% for the 6A8 control ($^*P < 0.003$ for all cases). **B–F:** Matrigel tube formation assays. Equal numbers of HDMVECs were seeded onto a matrigel support and incubated overnight with Vstat120-only CM (LN229Vstat120 or the HRGP control line 6A8), normal growth media (media only), or CM from three lines expressing both Vstat120 and HRGP (lines 5, 22, and 23.) With no CM added, after 14 hours some cells have begun to spread and form tube-like structures with an average of 12.7 branch points per 10× field (**F** – lane 1 – media only; 2 fields in each of 3 separate experiments were counted). This is reduced when Vstat120 is present in the original Vstat120 cell line or in the HRGP control line (6A8 – **E**) with 6.8 and 7.3 branch points counted for each (**F** – lanes 3 and 7). On addition of HRGP (**B–D**), increased numbers of web-like structures are observed consistent with tube formation. The average number of branch points was 18.2, 17.3, and 17.1 for the three HRGP lines 5, 22, and 23, respectively ($^*P < 0.002$ when compared with the control 6A8 line). HRGP attenuates Vstat120-induced apoptosis. **G:** Western blot of caspase-3 activation of HDMVECs after treatment with CMs containing either Vstat120 or Vstat120 and HRGP and quantification of caspase-3 activation (**H**). CMs with Vstat120 show a 2.5-fold (HRGP control 6A8) and fourfold (LN229Vstat120) increase in caspase-3 activation over serum-free media. When HRGP is present with Vstat120, caspase-3 activity returns to basal levels ($^*P < 0.04$ when comparing HRGP lines 5, 22, and 23 to the control line 6A8).

a measure of endothelial cell migration via movement of peripheral cells into the denuded area. HDMVECs were assayed for movement after 18 hours of exposure to CM with Vstat120 or Vstat120 plus HRGP. Under normal conditions (Figure 3A, media only – lane 1) with 5% serum in the media, cells have migrated into the acellular region from the edge of the scratched area with an average wound closure of 41%. When CM from parental LN229 cells was added (lane 2) the percent wound closure increased to 57%, likely attributable to promigratory growth factors produced and secreted from the tumor cell line. When Vstat120-containing CM from LN229Vstat120 (lane 3) or HRGP control 6A8 (lane 7) cells was added to the media (1:1 ratio) there was a distinct attenuation of migration consistent with previous observations.[14] Both CMs with added Vstat120 had an average wound closure of approximately 30%, one-half the closure area of the original LN229 line. Addition of CM from all three HRGP + Vstat 120-expressing lines, however, mitigated the Vstat120 effect (lanes 4, 5, and 6). When compared with the HRGP 6A8 control CM closure percentage (30%), all three HRGP-containing lines approximately doubled the closure area, effectively returning the percentage of cell migration to that of the original LN229 CM without Vstat120 present ($^*P < 0.003$ in all three cases).

These migration results were complimented by testing the CMs in a modified Boyden chamber assay (data not shown). When CM from the Vstat120-expressing LN229 glioma cell line was added to the HDMVECs, there was a marked reduction in overall migration, confirming previous observations.[11,14] This was also observed with Vstat120-containing CM from the cell line 6A8 transfected with the empty vector, whereas CM from all three HRGP + Vstat120-expressing lines (lines 5, 22, and 23) produced a dramatic increase in cellular migration when compared with vector controls, and even basic fibroblast growth factor alone. Therefore, HRGP not only reversed the inhibitory nature of Vstat120, but actually aided in a promigratory condition, possibly by inhibition of endogenous TSP produced by either the HDMVECs or the LN229 glioma line itself. Thus two different *in vitro* endothelial cell migration assays revealed that HRGP reversed the inhibitory activity of Vstat120 and even potentially provided additional promigratory effects.

We also tested the effects of HRGP and Vstat120 on the ability of HDMVECs to form three-dimensional tube-like structures when seeded onto matrigel, a laminin-rich basement membrane matrix (Figure 3B–F). The number of branch points within the endothelial cell layer was used as a measure of cell network formation. When me-

dia alone was added to the HDMVECs and incubated for 18 hours, significant tube formation was observed and an average of approximately 13 branches per field was counted (Figure 3F, media only – lane 1). An almost equivalent effect was seen with the LN229 parental line (LN229 – lane 2) with an average branch formation of 14 per field. When the Vstat120-rich CM from LN229Vstat120 (Figure 3F, lane 3) or from HRGP control 6A8 (Figures 3E, and 3F, HRGP control 6A8 – lane 7) cells was used, tube formation was significantly inhibited and the average branch numbers diminished to approximately seven per field. In contrast, CM from the three HRGP + Vstat120-expressing lines (Figure 3, B, C, D, and F - lanes 4, 5, and 6) induced increased tube formation and cellular network formation. The average branch number for these three lines was 18.1, 17.3, and 17.1, respectively – over 2.5 times greater than the HRGP 6A8 control (Compare – Figure 3F; $*P < 0.002$ for all three cases) and even greater than the LN229 CM absent of inhibitor. Taken together these studies demonstrate that HRGP can potently reverse the effects of Vstat120 *in vitro*.

Caspase-3 Activation Is Attenuated by HRGP Inhibition of Vstat120

Evidence suggests that TSP-1 and Vstat120 both engage CD36 via their TSR domains and that TSP-1 activates caspase-3 mediated apoptosis of endothelial cells.[9,11,24] Therefore, we tested whether Vstat120 could also induce apoptosis in a caspase-3–dependent manner and whether HRGP could attenuate this apoptotic signal. Both normal media with 10% serum as well as serum-free media added to HDMVECs induced little, if any, caspase-3 cleavage products (see Figure 3, G and H; normal media – lane 1 and serum-free – lane 2). The parental LN229 line showed minimal cleaved caspase-3 as well, approximately equal to the amount seen by serum-free media alone. When Vstat120 was produced in the CM of the HRGP control 6A8 line or the LN229Vstat120 line, a 2.5- to 4-fold increase in the canonical doublet of cleaved caspase-3 was observed (quantified in Figure 3H). Addition of HRGP to the CM, in all three cases, effectively attenuated the amount of cleaved caspase-3 back to basal levels ($*P < 0.04$ when comparing the three HRGP-producing lines to the control 6A8 line), suggesting that HRGP prevents Vstat120 from anti-angiogenic signaling, in part, by blocking caspase-3 activation.

HRGP Reverses the Anti-Angiogenic Activity of Vstat120 in Vivo

Previous studies showed that Vstat120 suppressed *in vivo* tumor growth in a dose-dependant manner via inhibition of tumor angiogenesis.[11,14] Because we have now shown that the HRGP CLESH domain physically interacts with Vstat120 and that addition of HRGP restores endothelial cell migration and tube formation in the presence of Vstat120, we hypothesized that HRGP would reverse the tumor growth inhibition and diminished tumor angiogenesis *in vivo* mediated by Vstat120-secreting tumors. We inoculated athymic nude mice with the LN229 glioma cells described above that expressed Vstat120 or Vstat120 + HRGP and monitored tumor volumes over a 50-day period. As previously reported for human LN229 glioblastoma cells, tumor growth over the initial 40 days was slow (average volume of <60 mm^3) and was similar for all lines tested. Beginning at approximately day 43, however, significant and dramatic differences in tumor growth were observed. The HRGP-expressing line 22 showed marked increase in mean tumor size and by day 50 had an average volume fivefold greater than that of the one Vstat120-expressing line 6A8 (Figure 4A, $*P < 0.0001$). This increase in tumor size was despite equivalent growth kinetics of these cells *in vitro* compared with 6A8 cells (Figure 2C). Line 23 showed an approximate twofold increase in tumor volume compared with 6A8, whereas line 5 had only slightly higher volumes than the control. The average amount of HRGP secreted by line 22 was approximately fivefold greater than by lines 5 and 23 (Figure 2B). These results are consistent with the hypothesis that increased HRGP expression attenuates the anti-angiogenic effects of Vstat120 and thus tumor growth attributable to decreased vascularity.

Increased Angiogenesis in HRGP-Expressing Tumors

To assess tumor vascularity, representative tumors from each line were harvested and vessel density examined by vWF staining. The control line 6A8 which secretes Vstat120 alone shows moderate vessel density (see Figure 4, B, C, and F) with an average of 10.9 vessels per 10× field. Two HRGP-containing lines showed similar vessel density and size to control with HRGP line 5 at 11.6 and HRGP line 23 slightly higher at 13.4 vessels counted per 10× field (a representative picture of these lines is shown in Figure 4D). The tumor line with 5× increased HRGP expression (HRGP line 22) showed a marked increase in vessel density (19.4 vessels per 10× field ($*P < 0.001$) as well as vessel size when compared with the other three groups (Figure 4, E and F). This suggests that increased expression of HRGP in these tumors may have a direct effects on tumor growth by allowing increased angiogenesis and vascular permeation.

HRGP Increases Orthotopic Brain Tumor Growth

We have recently shown that Vstat120 suppresses the growth of intracranial gliomas using multiple tumor lines.[11] To determine whether HRGP could reverse the anti-tumorigenic effects of Vstat120 within the brain, LN229V120 cells co-transfected with HRGP or control vector were orthotopically implanted into the brains of athymic mice ($n = 6$ mice per group). Excess cells were grown and analyzed by Western blot to confirm HRGP expression (Figure 5A). All three lines (5, 22, and 23) expressed HRGP with line 22 approximately a 5× greater

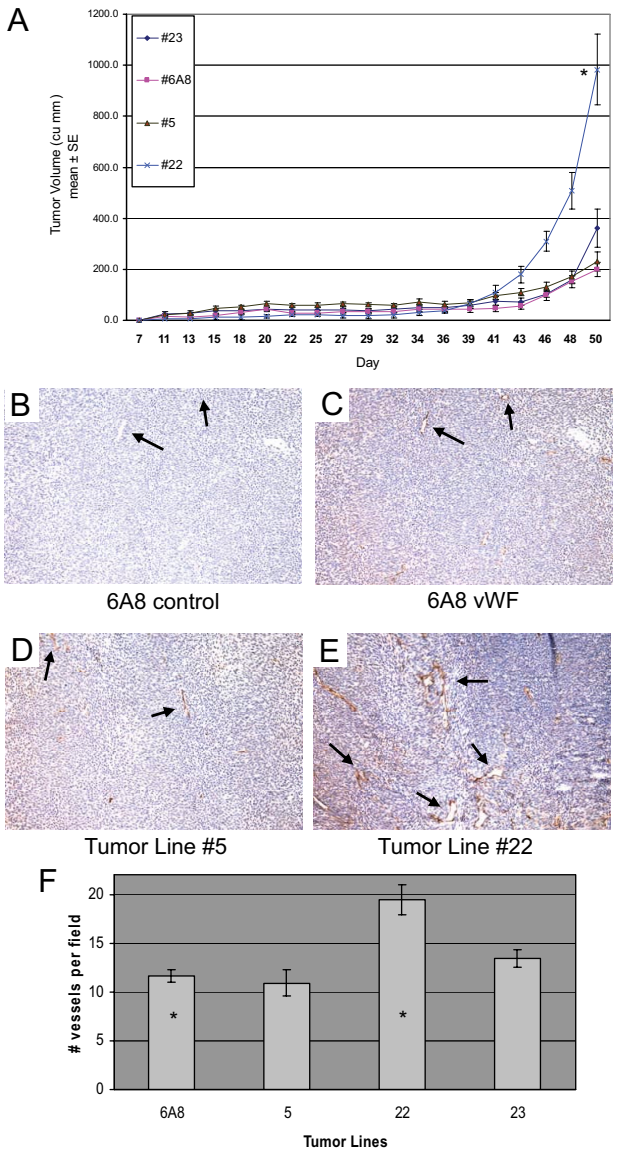

Figure 4. HRGP increases tumor growth and vascularity in Vstat120-expressing glioma cells transplanted subcutaneously into nude mice. **A:** Cloned cells that stably express both HRGP and Vstat120 (lines 5, 22, and 23) or Vstat120 alone (line 6A8) were injected subcutaneously into immunocompromised mice (n = 8 tumors per group) and tumor volumes were calculated over a seven-week period. Line 22, which expresses approximately 5× the amount of HRGP compared with lines 5 and 23, showed a rapid increase in tumor size from day 43 until sacrificed at day 50 due to tumor burden (*$P < 0.0001$ when comparing line 22 to control line 6A8). **B–F:** Increased vascularity in HRGP-expressing glioma tumors. Tumors from animals described in **A** were removed and paraffin sections processed and stained with monoclonal anti-vWF or control antiserum. Slides were developed with an HRP-conjugated avidin-biotin staining system and counterstained with hematoxylin. Matched regions of the tumors were used for vessel analysis. **Black arrows** show vWF-positive vessels stained brown from the DAB substrate. A representative field of a Vstat120-only expressing tumor (6A8, **B**) showed no apparent staining when control serum was added. The same field stained with vWF on an adjacent section showed small spread out vessels (**C**) that are quantified in **F**. HRGP-expressing tumor line 5 (**D**) and line 23 showed similar staining patterns to the Vstat120-only tumor (6A8), but HRGP line 22 shows a marked increase in vessel density and size when compared with the other lines (**E**). **F:** Vessels in each field were counted and plotted ±SEM (n ≥10 fields per group; *$P < 0.00003$ when comparing vessel number from line 22 and control line 6A8).

amount, consistent with protein analysis from previous cell passages. After 9 weeks, the animals were sacrificed and the brains removed. Ten-μm sections were cut ranging from 1 mm anterior to 1 mm posterior to the tumor injection site and stained. Sections with the largest tumor cross section area were used for relative measurements. Tumors are dense and the compact cells stain a dark purple with hematoxylin. The LN229 tumors without Vstat120 were large with an average volume approximately 40% of the injected hemisphere (Figure 5B – LN229 – lane 1). Tumors from brains injected with cells containing Vstat120 (line 6A8) were approximately one fourth the size (10% of hemisphere) of the LN229 control tumors (compare 5B – lanes 1 and 2). The tumor cells transfected with HRGP showed an increase in tumor area in all three lines tested (Figure 5B – lanes 3, 4, and 5) with lines 5 and 22 showing significance (*$P < 0.03$ and $P < 0.003$ respectively). Of note, the line with the highest level of HRGP expression (line 22) almost completely abrogated the Vstat120 anti-angiogenic effect (average tumor area 38% in LN229 control vs 32% tumor area in LN229Vstat120 HRGP line 22). Taken together, these studies show that HRGP is a potent inhibitor of Vstat120 induced anti-angiogenesis in brain tumors.

Increased Vessel Size and Density in Tumors Expressing HRGP

Sections of the tumor-containing mouse brains were analyzed for vessel growth by immunofluorescence microscopy. Serial sections to those used for hematoxylin and eosin staining were stained with anti-vWF antibody and viewed under a fluorescent microscope at ×40 magnification. Figure 5C shows an example of the vascularity of a control LN229 tumor absent of both Vstat120 and HRGP. In general, the vessels were moderate within the tumor near the surface of the brain with an increased number proximal to the injection point where it appears the tumor cells are intercalated with nontumorous cells. Therefore, areas at the intersection of the tumor and normal brain matter were used for vessel quantification. Tumors containing cells that express Vstat120 were generally smaller (see Figure 5B) with vessels that were both smaller in size and fewer in number (control line 6A8 had an average of 2.5 vessels per field – Figure 5, D and E, and quantified in 5I). When Vstat120 and HRGP were expressed simultaneously in these tumors an increase in both number and size of the vessels was observed (Figure 5, F, G, and H) in all three lines implanted. The average vessel number per field was approximately 4× that of the control 6A8 line (Figure 5I) with *$P < 0.001$ in all cases. The vascularity of these tumors was less than those of the original LN229 control tumors by about 50% yet significantly higher than tumors with Vstat120 alone, suggesting neovascularization as an important process needed for sustained tumor growth.

Increased HRGP Expression in Human Brain Tumors

Little is known of the effect of HRGP on human cancers. To address this issue we stained human brain tissue from normal subjects as well as from patients with grade IV

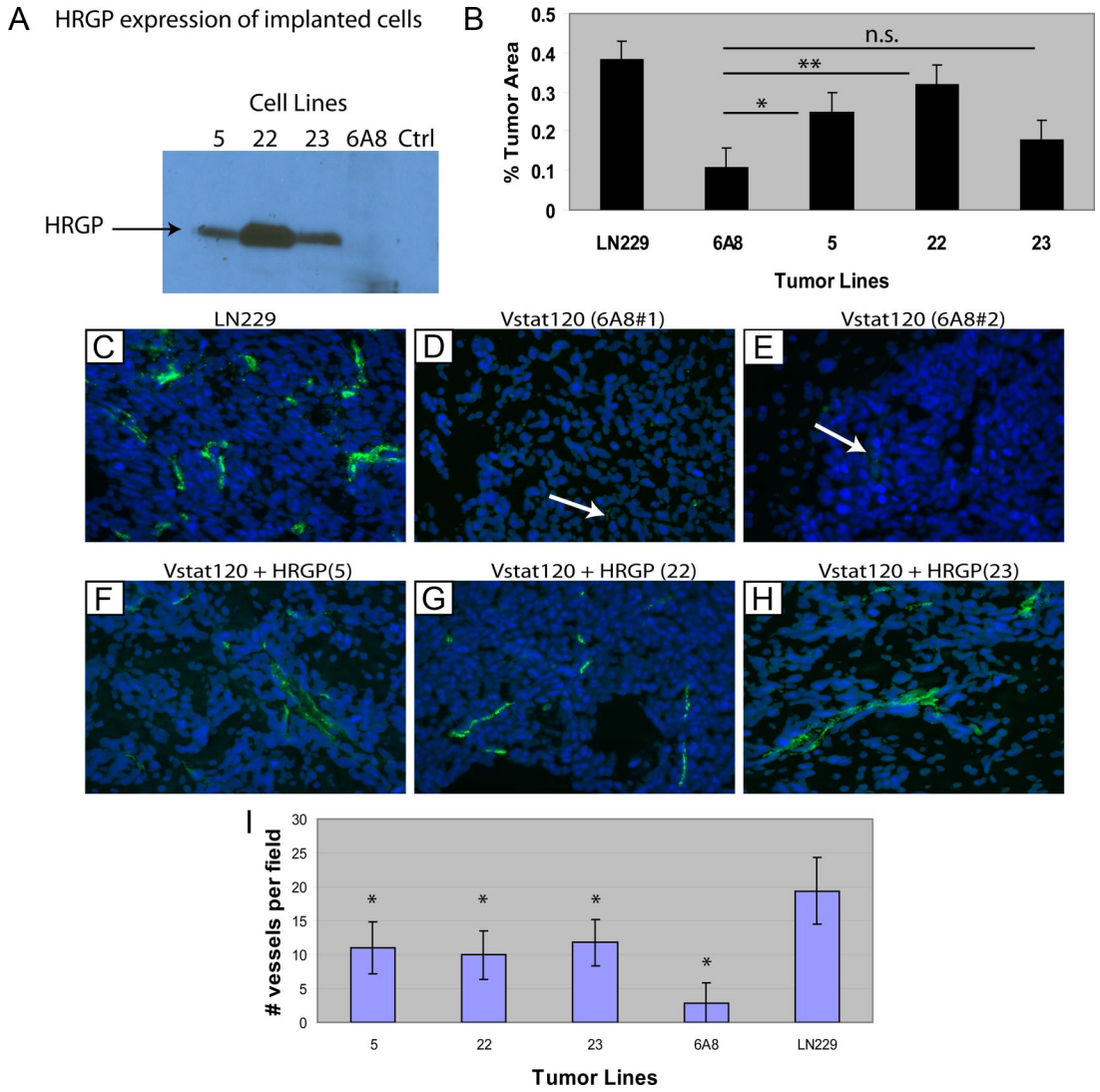

Figure 5. HRGP increases tumor growth in Vstat120-expressing glioma cells transplanted orthotopically into brains of nude mice. Cells from five LN229 cloned glioma cell lines (parental LN229, line 6A8 expressing Vstat120 alone, and lines expressing both Vstat120 and HRGP; lines 5, 22, and 23) were implanted into the brains of immunocompromised mice ($n = 6$ mice per group). **A:** Cells not used in the implantations were plated and tested for HRGP expression via Western blot. **B:** Quantification of the tumor area for each implanted group. Each section with the largest tumor area within 1 mm anterior to posterior of the injection point was used for analysis. To quantify, the area of tumor was calculated within the normal shape of the brain and any tumor area that expanded beyond that was not included. The percent tumor area represents the ratio of the measured tumor area/the area of the total hemisphere × 100%. Error bars are expressed as ±SEM. Significance was assessed by Student t test; $^{*}P < 0.03$, $^{**}P < 0.003$; n.s indicates not significant. **C–I:** HRGP increases vessel size and number in Vstat120 orthotopically implanted gliomas. Tumor sections were stained with anti-vWF and goat anti-rabbit alexa fluor 488 to visualize tumor vessels. Pictures were taken under ×40 magnification. The peripheral regions of each tumor that were in contact with the nontumorous tissue were used to calculate vessel density. Parental LN229 glioma line showed extensive blood vessel staining (green) within the tumor (cells stained blue with DAPI), especially at the tumor-brain tissue interface (**C**) with an average number of 19.4 per field (**I** – LN229 – lane 5). LN229 cells that stably express Vstat120 (control line 6A8 – representative images of two tumors are shown in **D** and **E**) showed dramatically reduced vessel number and size (**white arrows**). Vessel number per field was reduced to 2.8 in the presence of Vstat120 (**I** – 6A8 – lane 4). Tumors with both Vstat120 and HRGP constitutively expressed regain a significant amount of vascularity when compared with tumors with Vstat120 alone (**F–H**) with and average vessel density of 11, 9.9, and 11.8 per field (**I** – 5 – lane 1, 22 – lane 2 and 23 – lane 3) respectively. $^{*}P < 0.0001$ when comparing the HRGP lines with the control 6A8 line.

gliomas with a monoclonal anti-HRGP antibody. No specific staining was observed in either normal brain or GBM with nonimmune IgG control (Figure 6, C and D). In 25% (5/20) of the normal brain samples there was significant endothelial cell and basement membrane staining when compared with the IgG control (Table 1). In contrast, more than 83% of the GBM samples showed positive HRGP staining (15/18). This was much more intense than seen in the normal brains and was mainly located within the basement membrane (Figure 6, A and B, and Table 1). Using Fisher Exact test the differences in both incidence number and staining intensity were found to be statistically significant ($P = 0.0004$). For GBM tissue, the odds ratio of a positive HRGP expression was 15 (95% CI, 3,74) compared with normal brain tissue.

Discussion

The biology of proteins containing TSR repeats has been of great interest since the essential region for the anti-angiogenic effect of TSP-1 and TSP-2 on microvascular

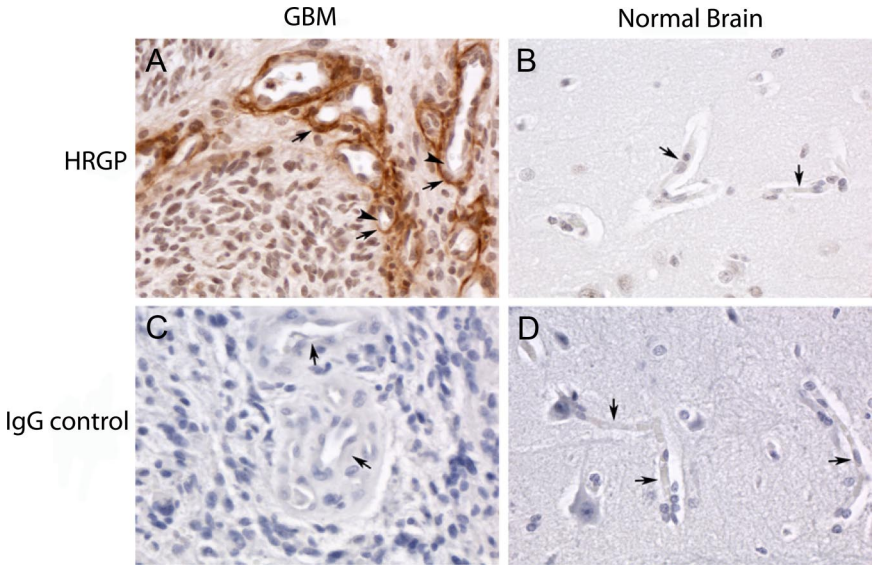

Figure 6. Formalin-fixed and paraffin-embedded biopsy sections of glioblastoma tumor (**A** and **C**) and of normal brain tissue removed during epilepsy surgery (**B** and **D**) were deparaffinized, blocked, and reacted with 0.7 μg/ml anti-HRGP antibody (**A** and **B**) or control IgG (**C** and **D**). This was followed by a biotin-conjugated secondary antibody, reaction with strepavidin, the DAB substrate, and hematoxylin counterstaining. Slides were viewed and photographed in a Leica DMR microscope at ×40 magnification. **Arrows** denote the basement membrane of blood vessels, and the **arrowheads** in panel **A** denote endothelial cells that are not stained with the anti-HRGP antibody. The tumor cells in the GBM biopsy are negative for HRGP staining.

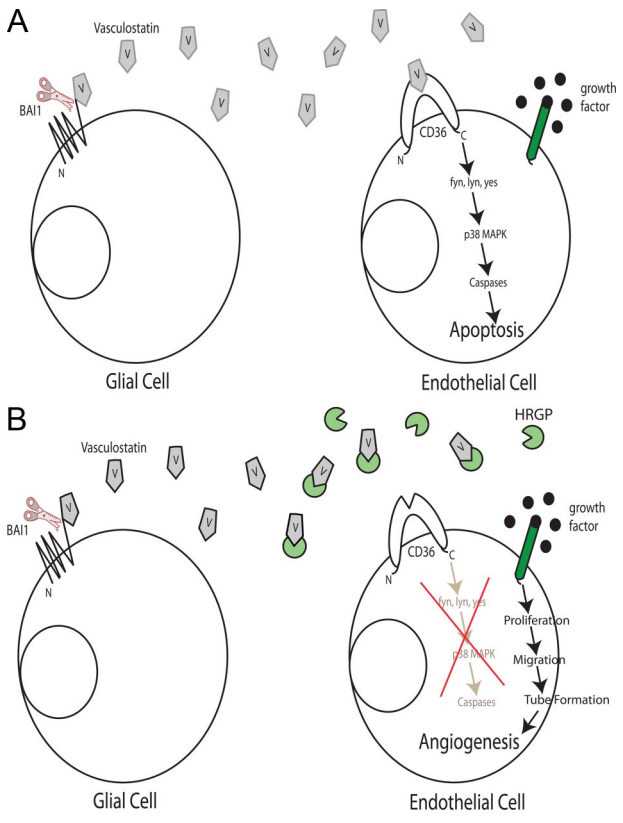

Figure 7. A and **B:** Model of the effect of Vstat120 on endothelial cells and the modulating role of HRGP. **A:** In the microenvironment of a brain tumor, growth factors such as basic fibroblast growth factor or vascular endothelial growth factor are secreted and induce angiogenesis via interaction with specific receptors on the vascular endothelium. At the same time, the extracellular domain of BAI1 is cleaved from the glial cell membrane liberating Vstat120 (V), which then interacts with the endothelial cell receptor CD36. Downstream signaling induced by CD36 through src kinases fyn and lyn and p38 MAP kinase diverts the pro-angiogenic growth factor signals to caspase-mediated apoptotic signals. **B:** As a consequence of vascular inflammation and/or increased permeability of the tumor neovessels induced by VEGF, plasma or platelet HRGP is deposited in the tumor bed where it acts as a decoy receptor for Vstat120. Vstat120 is then unable to bind its cell surface receptors and endothelial cell proliferation, migration, and tube formation occur, leading to increased vessel density and tumor growth.

endothelial cells was mapped to these domains. Over 70 human TSR-containing proteins have been identified.[25,26] Interestingly, the TSR domains have only been mapped to extracellular regions of integral membrane proteins or in proteins secreted into the extracellular space, with many being deposited into the matrix. This would suggest potential roles for the TSRs in cell–cell and cell–matrix interactions. A subset of TSR-containing proteins, including TSP-1, TSP-2, BAI1 (Vstat120), and ADAMTS-20 are potent inhibitors of angiogenesis, with the mechanism of at least three being dependent on interaction with CD36.

In our studies of CD36 structure/function relationships we discovered protein sequences homologous to the CD36 CLESH domain in several unrelated proteins known to bind TSP-1, including HIV gp120[17] and HRGP. We report here that the C-terminal CLESH domain of HRGP bound to Vstat120, whereas other HRGP domains, including an N-terminal domain with a lower degree of CLESH homology, did not. In multiple functional assays we also showed that HRGP reversed the actions of Vstat120 when both proteins were expressed concomitantly. These results are the first demonstration that HRGP can bind TSR-containing proteins other than thrombospondins, and suggest that HRGP may modulate activity of an entire class of angiogenesis inhibitors.

In vivo, HRGP exacerbated subcutaneous tumor growth when produced at a high enough concentration (Figure 4A). For tumors to rapidly increase in size, a disruption of the angiogenic balance to favor a pro-angiogenic phenotype is likely. In this instance, it is possible that increased tumor growth was supported when a threshold concentration of HRGP was reached, activating an angiogenic switch toward increased endothelial cell recruitment, enhanced angiogenesis, and rapid cell growth. As we reported previously, the average survival time of mice implanted in the brain with tumor cells secreting Vstat120 was significantly increased compared with animals injected with control cells, whereas tumor samples excised at equivalent time points expressing

Table 1. Expression of HRGP in Glioblastoma Tumor and Normal Brain

Tissue	Location	Intensity
Normal brain (n = 20)	EC/BM	1+ (5 of 20) Neg (15 of 20)
GBM (n = 18)	BM (occasional EC)	1+/2+ (15 of 18) Neg (3 of 18)

EC indicates endothelial cell; BM, basement membrane; GBM, glioblastoma tumor; HRGP, histidine-rich glycoprotein. Grading scale for staining: Neg, no staining; wk+, weak intensity staining; 1+, strong intensity staining; and 2+, very strong intensity staining, as compared with an IgG negative control. For a biopsy to be graded as wk+, 1+, or 2+ intensity staining, ≥10% of vessels in the tumor tissue were required to stain. The tumor cells in GBM biopsies were negative.

Vstat120 showed smaller tumor size and decreased vascularity compared with Vstat120 deficient tumors.[11]

In this report, glioma cell lines orthotopically implanted were even more responsive to HRGP than what was observed in the subcutaneous tumor model. Engineered lines producing HRGP dramatically inhibited the effect of Vstat120 resulting in increased tumor growth. Thus HRGP is a potent tumor promoting agent when present at sufficient levels and recruited to the tumor vasculature. This is supported by studies of human brain samples, which revealed significant increases in incidence and degree of HRGP expression in sections from aggressive gliomas compared with normal tumor-free controls. HRGP was found mainly in the basement membrane of the glioblastoma vasculature but was notably absent within the endothelial cells of the tumor. This complements the finding of Kaur et al who found that 35% of human GBMs tested stained positive for BAI1 (Vstat120).[12] They postulate that other factors are likely needed to overcome the angio-inhibitory functions of BAI1 for these tumors to grow. Our results show in the GBM tumors HRGP staining is clearly strongest in the areas of hypoxia adjacent to areas of tumor necrosis. There may be breakdown of the blood brain barrier in these areas and thus leakage of HRGP into the basement membrane. Vstat120 would thus be neutralized by binding to HRGP instead of the endothelial cell receptor CD36, and aggressive tumor growth would persist.

Interestingly, others have reported that HRGP potentially displays *anti*-angiogenic properties independent of thrombospondins or other TSR-containing proteins. Studies have shown the histidine/proline-rich region (HRR) region (Figure 1A) can be cleaved from the intact protein and elicit an anti-angiogenic response within larger endothelial cell types.[27–30] It is not unusual for fragments of proteins to display different properties than their parent molecule. In larger vessels, where CD36 is absent, the anti-angiogenic potential of the cleaved HRR region may prevail. In our studies within the microvasculature, however, we have not observed this effect.[21,22]

A schematic of the proposed Vstat120/CD36/HRGP angiogenic axis is shown in Figure 7, A and B. Under pro-angiogenic conditions within the brain, the presence of a stimulatory signal influences microvascular endothelial cells to be driven toward proliferation, migration and tube formation, eventually forming intact capillaries (Figure 7A). BAI1 is expressed on the surface of normal glial cells. The extracellular fragment of BAI1, Vstat120 (V), is released from the cellular membrane via proteolytic cleavage at a G protein–coupled receptor cleavage site.[14] It then can act as an anti-angiogenic agent by binding to the CLESH domain of CD36; this initiates an intracellular cascade involving fyn kinase, downstream MAP kinase signaling, caspase activation, and eventually apoptosis.[9] Vstat120 may also bind the surface of endothelial cells via $\alpha_v\beta_5$ integrin and initiate a second caspase mediated apoptosis pathway.[31] The end result is an inhibition of angiogenesis and potentially brain tumor growth.

Brain tumors may overcome the angiostatic function of Vstat120 by several different mechanisms. As previously shown, tumors could suppress expression of BAI1[12] or block release of Vstat120 from BAI1 by inhibiting cleavage at the GPS site.[14] Our data suggest a third mechanism by which tumors secrete or recruit the decoy HRGP to the site of the neoplasm (Figure 7B). Because tumor vessels are typically disorganized and "leaky" when compared with normal mature vessels and because HRGP is present in a moderately high concentration in blood, it is reasonable to hypothesize that HRGP could "leak" out of these hyperpermeable vessels into the surrounding tumor area. HRGP could also be released from activated platelets that have been mobilized to the tumor vasculature as part of an inflammatory or injury response. In fact, we previously demonstrated accumulation of HRGP and colocalization with TSP-1 in the matrix of human breast carcinoma.[21] Thus, tumors that produce HRGP or recruit it into their tumor bed potentially have a growth advantage via protection from TSP and other TSR-based therapeutic agents. An increase in the local concentration of HRGP could shift the angiogenic balance back to a pro-angiogenic phenotype, mitigating the effects of Vstat120 and other TSR-containing anti-angiogenic factors (such as TSP-1 and −2).

Thrombospondins have also been suggested to play an anti-angiogenic role at subpicomolar concentrations, independent of CD36, when the pro-angiogenic signal is nitric oxide (NO).[32] It would be interesting to determine whether Vstat120 can elicit the same effect within the brain and if HRGP can inhibit this process. Instances of aggressive tumor growth where increased amounts of TSPs are present, however, or the administration of TSR mimetic peptides as anti-angiogenic therapy would likely lessen the angiogenic effects of physiological NO and emphasize the TSP-CD36-HRGP angiogenic axis within the microvasculature.

Angiogenesis is a complex process that involves numerous cell types and regulatory systems. Perhaps the best understood natural anti-angiogenesis pathway is the microvascular homeostatic system mediated by the interaction of the transmembrane receptor CD36 with its ligands, TSP-1 and −2.[33] We recently showed for the first

time that a non-TSP protein containing multiple TSR domains (Vstat120) also influences angiogenesis via the CD36 system.[11,14] We now show using a combination of *in vitro* and *in vivo* approaches that HRGP, a circulating decoy for TSP-1 and −2, also functions as a decoy for this non-TSP TSR-containing protein, and thereby modulates the system to promote angiogenesis. We suggest that in conditions where neovasculature is poorly organized and "leaky," such as in tumor beds, or where platelet activation occurs, such as in a wound or inflammatory site, HRGP can accumulate in the extracellular matrix and abrogate the potent anti-angiogenic activity of a broad class of angiogenesis inhibitors.

References

1. Dvorak HF: Angiogenesis: update 2005. J Thromb Haemost 2005, 3:1835–1842
2. Ferrara N, Hillan KJ, Gerber HP, Novotny W: Discovery and development of bevacizumab, an anti-VEGF antibody for treating cancer. Nat Rev Drug Discov 2004, 3:391–400
3. Kim KJ, Li B, Winer J, Armanini M, Gillett N, Phillips HS, Ferrara N: Inhibition of vascular endothelial growth factor-induced angiogenesis suppresses tumour growth in vivo. Nature 1993, 362:841–844
4. Patel SN, Serghides L, Smith TG, Febbraio M, Silverstein RL, Kurtz TW, Pravenec M, Kain KC: CD36 mediates the phagocytosis of Plasmodium falciparum-infected erythrocytes by rodent macrophages. J Infect Dis 2004, 189:204–213
5. Iruela-Arispe ML, Lombardo M, Krutzsch HC, Lawler J, Roberts DD: Inhibition of angiogenesis by thrombospondin-1 is mediated by 2 independent regions within the type 1 repeats. Circulation 1999, 100:1423–1431
6. Reiher FK, Volpert OV, Jimenez B, Crawford SE, Dinney CP, Henkin J, Haviv F, Bouck NP, Campbell SC: Inhibition of tumor growth by systemic treatment with thrombospondin-1 peptide mimetics. Int J Cancer 2002, 98:682–689
7. Tolsma SS, Volpert OV, Good DJ, Frazier WA, Polverini PJ, Bouck N: Peptides derived from two separate domains of the matrix protein thrombospondin-1 have anti-angiogenic activity. J Cell Biol 1993, 122:497–511
8. Iruela-Arispe ML, Luque A, Lee N: Thrombospondin modules and angiogenesis. Int J Biochem Cell Biol 2004, 36:1070–1078
9. Jimenez B, Volpert OV, Crawford SE, Febbraio M, Silverstein RL, Bouck N: Signals leading to apoptosis-dependent inhibition of neovascularization by thrombospondin-1. Nat Med 2000, 6:41–48
10. Dawson DW, Pearce SF, Zhong R, Silverstein RL, Frazier WA, Bouck NP: CD36 mediates the In vitro inhibitory effects of thrombospondin-1 on endothelial cells. J Cell Biol 1997, 138:707–717
11. Kaur B, Cork SM, Sandberg EM, Devi NS, Zhang Z, Klenotic PA, Febbraio M, Shim H, Mao H, Tucker-Burden C, Silverstein RL, Brat DJ, Olson JJ, Van Meir EG: Vasculostatin inhibits intracranial glioma growth and negatively regulates in vivo angiogenesis through a CD36-dependent mechanism. Cancer Res 2009, 69:1212–1220
12. Kaur B, Brat DJ, Calkins CC, Van Meir EG: Brain angiogenesis inhibitor 1 is differentially expressed in normal brain and glioblastoma independently of p53 expression. Am J Pathol 2003, 162:19–27
13. Fukushima Y, Oshika Y, Tsuchida T, Tokunaga T, Hatanaka H, Kijima H, Yamazaki H, Ueyama Y, Tamaoki N, Nakamura M: Brain-specific angiogenesis inhibitor 1 expression is inversely correlated with vascularity and distant metastasis of colorectal cancer. Int J Oncol 1998, 13:967–970
14. Kaur B, Brat DJ, Devi NS, Van Meir EG: Vasculostatin, a proteolytic fragment of brain angiogenesis inhibitor 1, is an antiangiogenic and antitumorigenic factor. Oncogene 2005, 24:3632–3642
15. Crombie R and Silverstein R: Lysosomal integral membrane protein II binds thrombospondin-1. Structure-function homology with the cell adhesion molecule CD36 defines a conserved recognition motif J Biol Chem 1998, 273:4855–4863
16. Pearce SF, Roy P, Nicholson AC, Hajjar DP, Febbraio M, Silverstein RL: Recombinant glutathione S-transferase/CD36 fusion proteins define an oxidized low density lipoprotein-binding domain. J Biol Chem 1998, 273:34875–34881
17. Crombie R, Silverstein RL, MacLow C, Pearce SF, Nachman RL, Laurence J: Identification of a CD36-related thrombospondin 1-binding domain in HIV-1 envelope glycoprotein gp120: relationship to HIV-1-specific inhibitory factors in human saliva. J Exp Med 1998, 187:25–35
18. Jones AL, Hulett MD, Parish CR: Histidine-rich glycoprotein: a novel adaptor protein in plasma that modulates the immune, vascular and coagulation systems. Immunol Cell Biol 2005, 83:106–118
19. Engesser L, Kluft C, Briet E, Brommer EJ: Familial elevation of plasma histidine-rich glycoprotein in a family with thrombophilia. Br J Haematol 1987, 67:355–358
20. Kuhli C, Scharrer I, Koch F, Hattenbach LO: Recurrent retinal vein occlusion in a patient with increased plasma levels of histidine-rich glycoprotein. Am J Ophthalmol 2003, 135:232–234
21. Simantov R, Febbraio M, Crombie R, Asch AS, Nachman RL, Silverstein RL: Histidine-rich glycoprotein inhibits the antiangiogenic effect of thrombospondin-1. J Clin Invest 2001, 107:45–52
22. Simantov R, Febbraio M, Silverstein RL: The antiangiogenic effect of thrombospondin-2 is mediated by CD36 and modulated by histidine-rich glycoprotein. Matrix Biol 2005, 24:27–34
23. Liang CC, Park AY, Guan JL: In vitro scratch assay: a convenient and inexpensive method for analysis of cell migration in vitro. Nat Protoc 2007, 2:329–333
24. Volpert OV, Zaichuk T, Zhou W, Reiher F, Ferguson TA, Stuart PM, Amin M, Bouck NP: Inducer-stimulated Fas targets activated endothelium for destruction by anti-angiogenic thrombospondin-1 and pigment epithelium-derived factor. Nat Med 2002, 8:349–357
25. Tucker RP: The thrombospondin type 1 repeat superfamily. Int J Biochem Cell Biol 2004, 36:969–974
26. de Fraipont F, Nicholson AC, Feige JJ, Van Meir EG: Thrombospondins and tumor angiogenesis. Trends Mol Med 2001, 7:401–407
27. Juarez JC, Guan X, Shipulina NV, Plunkett ML, Parry GC, Shaw DE, Zhang JC, Rabbani SA, McCrae KR, Mazar AP, Morgan WT, Donate F: Histidine-proline-rich glycoprotein has potent antiangiogenic activity mediated through the histidine-proline-rich domain. Cancer Res 2002, 62:5344–5350
28. Olsson AK, Larsson H, Dixelius J, Johansson I, Lee C, Oellig C, Bjork I, Claesson-Welsh L: A fragment of histidine-rich glycoprotein is a potent inhibitor of tumor vascularization. Cancer Res 2004, 64:599–605
29. Vanwildemeersch M, Olsson AK, Gottfridsson E, Claesson-Welsh L, Lindahl U, Spillmann D: The anti-angiogenic His/Pro-rich fragment of histidine-rich glycoprotein binds to endothelial cell heparan sulfate in a Zn2+-dependent manner. J Biol Chem 2006, 281:10298–10304
30. Dixelius J, Olsson AK, Thulin A, Lee C, Johansson I, Claesson-Welsh L: Minimal active domain and mechanism of action of the angiogenesis inhibitor histidine-rich glycoprotein. Cancer Res 2006, 66:2089–2097
31. Koh JT, Kook H, Kee HJ, Seo YW, Jeong BC, Lee JH, Kim MY, Yoon KC, Jung S, Kim KK: Extracellular fragment of brain-specific angiogenesis inhibitor 1 suppresses endothelial cell proliferation by blocking alphavbeta5 integrin. Exp Cell Res 2004, 294:172–184
32. Isenberg JS, Ridnour LA, Dimitry J, Frazier WA, Wink DA, Roberts DD: CD47 is necessary for inhibition of nitric oxide-stimulated vascular cell responses by thrombospondin-1. J Biol Chem 2006, 281:26069–26080
33. Simantov R, Silverstein RL: CD36: a critical anti-angiogenic receptor. Front Biosci 2003, 8:s874–s882